Aeolian Research 19 (2015) 183–194

Contents lists available at ScienceDirect

Aeolian Research

journal homepage: www.elsevier.com/locate/aeolia

In-situ measurement of dust devil activity at La Jornada Experimental Range, New Mexico, USA

Ralph D. Lorenz [a,*], Lynn D. Neakrase [b], John D. Anderson [c]

[a] Johns Hopkins University Applied Physics Laboratory, 11100 Johns Hopkins Road, Laurel, MD 20723, USA
[b] Department of Astronomy, New Mexico State University, Las Cruces, NM, USA
[c] La Jornada Experimental Range, Las Cruces, NM, USA

ARTICLE INFO

Article history:
Received 11 October 2014
Revised 4 January 2015
Accepted 5 January 2015
Available online 1 April 2015

Keywords:
Dust devils
Meteorology
Power law
Vortex structure

ABSTRACT

We document observations of dust devil vortices using a linear array of 10 miniature pressure- and sunlight-logging stations in summer 2013 at La Jornada Experimental Range in the southwestern USA. These data provide a census of vortex and dust-devil activity at this site. The simultaneous spatially-distributed measurements resolve the horizontal pressure structure of several dust devil encounters, and the data can be fit well with an analytic model, giving independent measures of vortex size and intensity.

1. Introduction

Dust devils are an important agent of dust-raising on Earth and Mars, and are responsible for occasional, even fatal, accidents. Thus it is important that their frequency be understood. Like other atmospheric vortices, dust devils are associated with a local air pressure drop. In addition to being a convenient measure of the overall intensity of a dust devil (as is also the case with other vortex motions such as tornados), the pressure drop may itself play a significant role in dust-lifting (e.g., Balme and Hagermann, 2006). Temporary pressure drops associated with dust devils, much like those of tornados (e.g., Karstens et al., 2010), have been long observed on Earth (e.g., Wyett, 1954; Lambeth, 1966; Sinclair, 1973; Lorenz, 2012a), without being systematically surveyed. In fact such pressure drops are actually better documented in studies of dust devils on Mars (e.g., by Mars Pathfinder: Murphy and Nelli, 2002, and by the Phoenix mission, Ellehoj et al., 2010), where landers have recorded meteorological parameters over long periods with a high enough cadence to detect small vortical structures. Terrestrial records from fixed stations are not generally made in dust-devil-prone areas with sufficiently rapid sampling (~1 Hz or better is typically required) to resolve dust devils. New pressure-logging instrumentation (Lorenz, 2012b) has now permitted efficient terrestrial surveys, with several hundred events captured in a month at El Dorado playa in Nevada (Lorenz and Lanagan, 2014). Here we report observations made some 850 km distant, at La Jornada Experimental Range, New Mexico. This investigation helps establish how typical or otherwise the El Dorado observations may have been.

While single-station observations are useful to characterize the level of activity at a site overall, there are significant ambiguities in interpreting the pressure history alone at one location. In particular, the miss distance (i.e. distance between the station and the center of the vortex at its closest approach) is not known, and while analysis of duration and pressure drop of many events can shed some light on possible correlations between diameter and intensity (core pressure drop) by assuming that miss distances are uniformly distributed (e.g., Lorenz, 2014), it would desirable, especially where only limited survey time is available, to determine the horizontal structure of vortices directly by making simultaneous measurements at many stations. We describe here some preliminary experiments in this direction in summer 2013, with a linear array of 10 pressure loggers.

Finally, it has been suggested that, on Mars at least, many more dustless vortices are present than dust devils. No systematic data is presently available to probe this question on Earth. However, the linear array of pressure loggers we deployed were equipped with small solar cells which record the incident sunlight on each station. Reduction (or in some instances, an increase) in the solar cell current provides information on the dust loading associated with a vortex whose presence is indicated by a pressure drop.

* Corresponding author. Tel.: +1 443 778 2903; fax: +1 443 778 8939.
E-mail address: Ralph.lorenz@jhuapl.edu (R.D. Lorenz).

http://dx.doi.org/10.1016/j.aeolia.2015.01.012
1875-9637/

2. Instrumentation

Although a variety of criteria can be applied to infer the presence of a vortex (which may or may not be heavily dust-laden) such as wind intensification and temperature perturbation, the most consistent and robust signatures (e.g., Ringrose et al., 2007) are a veer in wind direction, and pressure drop. The latter is convenient to measure in the field, and has two characteristic quantities, peak drop and width, which are generally easy to quantify. We use Gulf Coast Data Concepts B1100 pressure loggers, which monitor a precision Bosch BMP085 pressure sensor (logged with a resolution of 1 Pa, or 0.01 mb) with a microcontroller that logs the pressure data and housekeeping temperature as ASCII files on a 2 GB microSD flash memory card. The whole unit operates as, and its form factor resembles, a large USB memory stick, facilitating data transfer to a PC. As described in Lorenz (2012b), for this application the nominal single AA battery is replaced by a pair of alkaline D-cells, allowing unattended multi-month operation at sample rates of 2 Hz or more. The sensor and battery are installed in a plastic case, drilled to allow pressure equalization and painted a light brown to minimize visible signature and reduce the heating of the black plastic.

An augmentation to the standard B1100 that was made available to us by the manufacturer is the option to record an additional analog voltage (0–5 V) at an interval of 1 s. As discussed in Lorenz and Jackson (2015) a convenient application of this channel is a small solar cell with a parallel resistor, wired to record the photocurrent as a measure of sunlight intensity and thus dust obscuration.

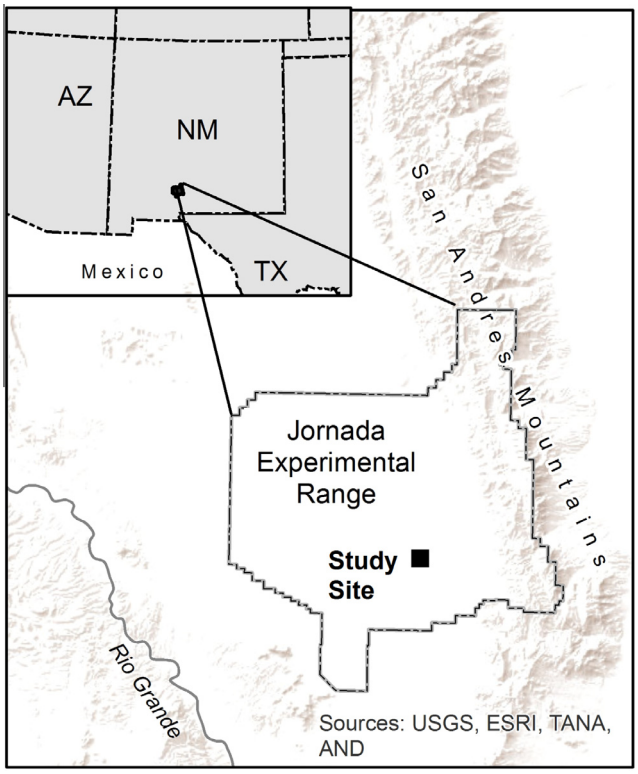

Fig. 1. Location map.

3. Site and observation period

Prior surveys have been conducted at El Dorado playa in Nevada, an open site where various recreational pursuits (drag-racing, model aircraft flying, etc.) are conducted and some attrition of even somewhat camouflaged instrumentation has been encountered. In contrast, the Jornada Experimental Range is a facility where public access is controlled, and instrumentation can be left deployed in the open without substantial fear of unauthorized removal. This allowed us to leave a linear array of stations unattended for several months.

The Jornada Experimental Range (783 km^2) lies 37 km north of Las Cruces, NM on the Jornada del Muerto Plain in the northern part of the Chihuahuan Desert (see Fig. 1). The Jornada is typical of the Basin and Range province of the American Southwest and is located between the Rio Grande floodplain (elevation 1186 m) on the west and the crest of the San Andres Mountains (2833 m) on the east. Just beyond the San Andres mountains are the dunes of White Sands National Monument, and the nearby missile range, which was the site of a visual dust devil survey 30 years ago (Snow and McClelland, 1990).

The climate of Jornada is characteristic of the northern region of the Chihuahuan desert with abundant sunshine, low relative humidity, wide ranges of daily temperature (average highs are 36 °C in June), and variable precipitation both temporally and spatially. Potential evaporation is approximately 10 times the average precipitation, which is ~241 mm yr^{-1} and occurs as localized thunderstorms during July, August, and September.

A further advantage is that the site is very well-documented in terms of weather, with nearby meteorological stations, and in the properties of the ground and vegetation, which can influence dust-lifting. The nearest generally-available meteorological data is at a SCAN (Soil Climate Analysis Network) tower a couple of km to the south.

An exploratory survey with a single station in summer 2012 indicated that a useful encounter rate could be expected. The data from that station are not reported here (while a number of detections were made, this initial deployment suffered high pressure noise levels due to inadequate temperature compensation in the logger configuration – see Lorenz (2012b)). On the basis of those data, an array of 10 loggers was deployed in mid-May 2013 (see Fig. 2). The site was chosen for convenient road access and the proximity of an existing installation. Several months of data were expected.

It was understood from informal reports that the predominant wind direction was north–south, and thus it was assumed that dust devils would generally translate in that direction. Accordingly the array was aligned roughly east–west (in fact about 30° north of east – see Fig. 3). Since it was expected that the dominant dust devil diameter might be only a few meters, the loggers were spaced 4 m apart (see Fig. 3). The ground was somewhat hard-caked at the deployment, suggesting dust may not be readily lifted.

4. Dust devil events detection and analysis

Surprisingly, when the loggers were retrieved in September 2013, water and mud were found to have intruded into almost all of them. (The logger units of course could not be sealed since they measure an air pressure signal.) This appears to have been a result of monsoon rainstorms at the end of June. The loggers all ceased recording on June 30, when the nearby SCAN tower indicates 0.4 inches of rain. The effective observing period was 45 days.

Most of the loggers, many with their circuit boards caked with mud, failed to respond directly to download commands via their USB interface. However, in all but one instance data could be recovered by removing the small micro-SD memory card from the logger, cleaning its connectors, and inserting into a functioning unit that had been kept in the laboratory.

Station S22 failed to provide any data. The data from station S29 is unaccountably noisier than the others, but is still usable. Solar

Fig. 2. Configuration of the array, image courtesy of Google Earth. The GPS location of S29 appears slightly inaccurate – its separation from S28 was similar to the other spacings (see Fig. 3). The dirt road providing access is visible at lower left; an instrumentation tower and square fence is visible in the center.

Fig. 3. Field photograph of the array configuration. The logger boxes are approximately 20 cm long, spaced by about 4 m. Note that the surface is partly grass-covered.

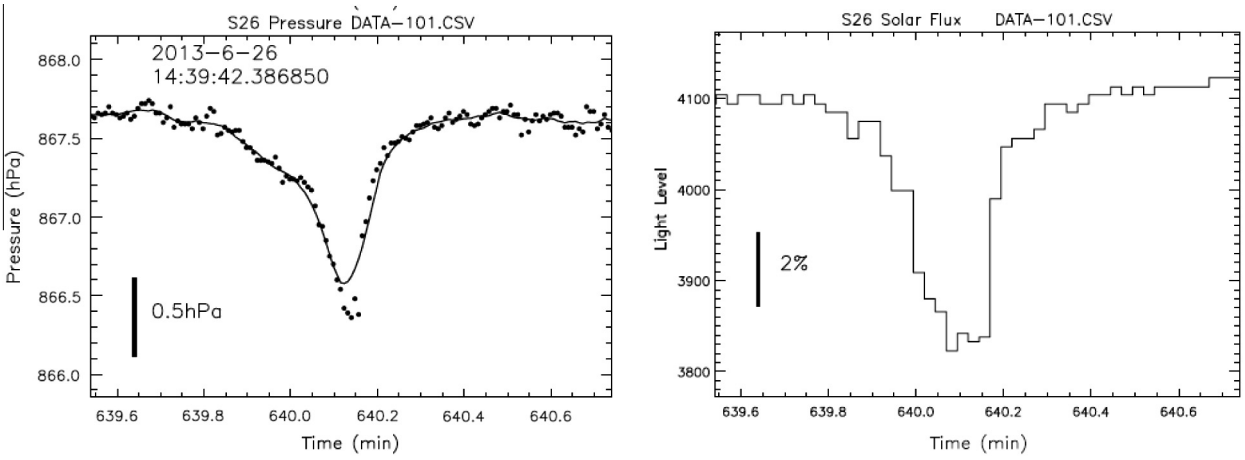

Fig. 4. Example event – 0.4 mbar pressure drop lasting about 10 s is a clear vortex signature. The points are individual pressure records at 2 Hz and have a characteristic scatter of ~0.2 mbar, probably largely due to digitization noise since points are clustered. The solid line is a simple 10-point running mean. This vortex event is accompanied by a ~7% drop in sunlight, indicating the vortex was dust-laden. Note that the peak attenuation of sunlight occurs just before minute 641.0 (the time axis is time since the start of a 12-h data record) whereas the peak pressure drop is shortly afterwards. This suggests the dust devil moved from the sunward direction.

flux data was available from station S24 only for part of the record, then read zero thereafter as the logger became physically inverted, perhaps due to bovine activity.

Devils were identified by examining the pressure record with a script to compute the difference between a local 6-s average, and an average of similar periods 30 s before and after that window (see Lorenz and Jackson, 2015). When this difference exceeded a threshold of 20 Pa and 4 times the root-mean-squared fluctuation in the before- and after-periods, a vortex event was recorded. This is a somewhat strong criterion, but yields a low false-positive rate. About twenty events were detected in each dataset – one example is shown in Fig. 4.

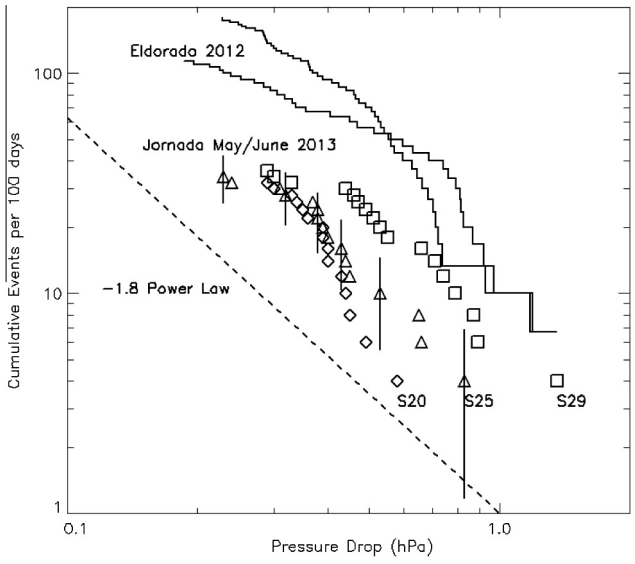

Fig. 5. A cumulative frequency plot of vortex events detected at stations S20, S25 and S29 (diamonds, triangles and squares respectively). The lowest, rightmost point in each set is the single largest (peak pressure drop) event in the record. The vertical lines indicate N^0.5 error bars. It is seen that the population seen by each station are similar but slightly displaced due to most events being common to all three, but with several additional detections in S25 and S29. The data are distributed consistently with a power law with a (cumulative) exponent of −1.8 (dashed line), with possibly a steeper fall-off at the largest size. The population shape is similar to that observed the previous year at the Eldorado playa site in Nevada by Lorenz and Lanagan (2014) shown by the staircase solid lines.

The solar cell signal is in principle a useful measure of cloudiness, since cloud shadows cause often rapid drops in current. For this reason, however, the solar flux is a poor detector of dust devils in that it has too high a false alarm rate. Rather, we identify vortices in the pressure record and assess the solar data only in the context of vortex events.

5. Results and Discussion

5.1. Vortex population

Since the loggers are so closely spaced, the amount of independent information on the population of devils is much less than 10 times a single logger. We demonstrate for consistency the populations indicated by the two loggers at each end of the array (S20 and S29) and one in the middle (S25). As Fig. 5 shows, the cumulative distributions of peak pressure drop are similar in shape, although there appears to be an interestingly consistent increase from S20 to S25 to S29 in number of events detected. This presumably indicates some terrain effect, perhaps due to topography, thermal inertia, dust availability and/or aerodynamic roughness. S29, with the largest number of detections, is furthest from the road. The variation here, of a factor of a few over only a few tens of meters, is striking; a similar factor of two-to-several difference between stations ~1 km apart on a Nevada playa was noted by Lorenz and Jackson (2015). This terrain dependence will be an interesting subject of future study.

On these logarithmic axes, the data are reasonably described by a power law with an exponent of −1.8 (i.e. a differential power law of −2.8, not too different from the distribution observed at Mars – Lorenz (2012a)). There appears, as in a survey at Eldorado playa in Nevada the previous summer (Lorenz and Lanagan, 2014) to be some convexity of the distribution, with numbers falling off somewhat more steeply at the largest sizes. It is notable that the rate of detections appears about 3 times lower than for Eldorado in 2012, although it should be noted that the counts there by Lorenz and Lanagan (2014) were made by manual inspection of the data, which yields more detections (at the cost of more analysis effort, which would be prohibitive for large arrays of sensors) than the automatic procedure described above.

Data from station S26 is given in Table 1. It may be noted that most of the events were detected while the datalogger had a temperature between 40 °C and 50 °C – clearly such observations

Table 1
Dust devil events recovered on station S26. The local date and time are indicated by columns MDHMS (month, day, hour, minute, second). The temperature is not the air temperature but the temperature of the datalogger. ΔP1 is the difference between 0.1 min average pressures used as the detection criterion (>0.2 mbar for detection), ΔP2 is the maximum pressure excursion in the record (i.e. the peak datapoint in the event) and ΔP3 is the amplitude of a Gaussian fit to the event. The duration is the width of that Gaussian fit. The light level is in arbitrary units, but peaks at about 4400 at summer noon on a clear day. The drop in light level is computed from the light level at the start of the event.

File#	Min	M	D	H	M	S	Pressure (mbar)	Temp (°C)	ΔP1	ΔP2	ΔP3	Duration (s)	Light level	Drop (%)
20	125.69	5	16	16	59	3	859.94	46.8	0.76	0.78	0.8	12	4094	0.33
20	169.05	5	16	17	42	24	860.97	46.4	0.25	0.43	0.31	10	3754	0.61
29	567.52	5	21	12	28	14	790.05	12.6	0.21	0.15	0.4	5	3378	2.39
40	193.15	5	26	18	22	51	845.59	47.1	0.34	0.47	0.43	1	2145	0
41	665.13	5	27	14	15	39	864.81	12.7	0.26	0.29	0.43	13	4390	0
43	625.2	5	28	13	37	21	852.86	12.0	0.36	0.37	0.78	6	4062	0.19
46	90.2	5	29	16	44	48	868.21	42.9	0.37	0.63	0.54	5	4094	1.16
50	32.69	5	31	15	50	34	863.34	51.9	0.38	0.41	0.38	18	4164	0.21
59	582.53	6	5	13	7	46	839.3	17.5	0.28	0.34	0.31	22	3760	0
60	120.07	6	5	17	26	8	850.08	50.2	0.33	0.56	0.34	12	3849	0
60	234.64	6	5	19	20	42	834.31	50.5	0.24	0.52	0.31	7	2659	0.16
68	25.5	6	9	15	58	6	969.01	54.2	0.21	0.19	0.28	6	4069	0.02
75	591.66	6	13	13	29	58	895.32	26.2	0.23	0.23	0.36	8	3721	0.77
76	12.17	6	13	15	51	18	866.81	53.8	0.44	0.62	0.53	32	4079	0.13
86	101	6	18	17	28	18	853.28	48.2	0.45	0.68	0.57	9	4279	0.17
90	74.19	6	20	17	4	45	855.03	50.6	0.35	0.41	0.41	8	2365	30.5
90	235.02	6	20	19	45	35	841.49	50.7	0.29	0.52	0.34	14	877	1.1
93	685.57	6	22	15	18	35	884.24	19.1	0.28	0.41	0.3	11	3828	0
96	140.61	6	23	18	16	4	851.32	48.8	0.26	0.37	0.3	30	3401	0
97	656.2	6	24	14	52	28	801.01	20.0	0.29	0.38	0.37	9	4179	0.38
100	166.55	6	25	18	45	17	847.36	49.2	0.31	0.56	0.41	8	3052	0
101	640.14	6	26	14	39	42	848.76	15.3	0.72	1.26	1.07	7	4053	3.48
101	708	6	26	15	47	34	939.07	15.3	0.27	0.46	0.4	8	4142	0.15
102	49.58	6	26	16	49	57	868.11	53.0	0.34	0.54	0.38	11	3973	0.11
109	654.08	6	30	15	0	10	863.85	25.7	0.31	0.59	0.52	6	3889	0.2

impose rigors on instrumentation. It may also be noted that events are not randomly distributed in time – with 24 events distributed across 45 days, it is somewhat surprising that two days have three events each. In other words, there are some favorable times and some unfavorable times, so the overall event rate reflects a dilution of the peak occurrence rate.

5.2. Array measurements

A novel element in the research described here is the use of a linear array of sensors to record the horizontal structure of vortex structures. The only prior effort of which we are aware that attempts anything similar is that by Lambeth (1966) almost a half-century ago, using manually-triggered chart recorders on an array of six stations at White Sands Missile Range, about 80 km to the Northeast of the present site. That work reported a modest number of encounters, but did not offer much detail on the horizontal variation of any given event. A single horizontal structure measurement was reported by Lorenz (2008) in an antecedent effort to the present one, using stations which had only memory capacity to record about 1 h of measurements. While that effort demonstrated the concept, the short measurement duration (limited to ~8000 samples), and the slow transfer of data via a serial datalink, made the hardware impractical for long duration surveys. The dramatic advances in flash memory (allowing tens of millions of samples) now make multi-week operations viable, and able to capture statistically-useful numbers of encounters with a single deployment and retrieval. The use of a simple ASCII file system for the data records, and the rapid drag-and-drop transfer of data via USB, make it possible to handle the much larger volumes of data in an efficient way.

Key to constructing a useful array dataset is the synchronization of records between stations. Each logger has a realtime clock, set via a configuration file read when the logger boots upon disconnection from the USB port on a PC. The clock-setting operation is usually accurate to within a few seconds, and all loggers were initialized from the same PC over the span of about half an hour. Crystal-controlled clocks can exhibit drift of many seconds per month, especially when subject to the extreme temperature fluctuations in the present application (with dataloggers exposed to the sun and reaching 50 °C – see Table 1), so the intrinsic co-registration of the loggers progressively degrades somewhat and in a few cases, the clock was found to have failed. However, because all loggers were started at approximately the same time, with the same 2 Hz sample rate and record size (86,400 samples, or 12 h), simply referring to the same file number for each logger, and the same number of minutes from the start of that file, gave synchronization to about 1 min, and an ad-hoc correction shift for each logger could be estimated. In future work, it may be possible to automate this process by simple cross-correlation of records.

Using events identified by hand, or from the autodetection algorithm described earlier, records from the whole array were inspected, and a number of examples follow.

Fig. 6 shows a rather ideal example, where a clean pressure dip is observed, correlated directly with a solar flux dip, showing that the vortex was dust-bearing. Furthermore, the strongest dip is seen at the center of the array, falling off to each side. It may be noted that the profile is asymmetric – the attack is shallower and longer than the decay. This is a not uncommon feature and may be characteristic of the interaction of a vortex with the wind field that advects it.

Fig. 7 shows an encounter with a fairly narrow devil – the raw signature is less than 10 s long, but is rather intense, with a ~1 mb core pressure drop at S27 (such large pressure drops are encountered only about once per 20 days). It is notable that the obscuration signal has a pronounced double dip, suggesting a well-defined dust wall with a clear central region. The wall causes a solar flux drop of only 2%, suggesting a ~0.02 optical depth. The two westernmost stations record a larger, single dip than the rest, suggesting either a greater local dust availability and/or some azimuthal structure to the dust devil.

Fig. 8 shows an encounter with a pair of devils, or possibly a single devil with a cycloidal migration path that leads to two close

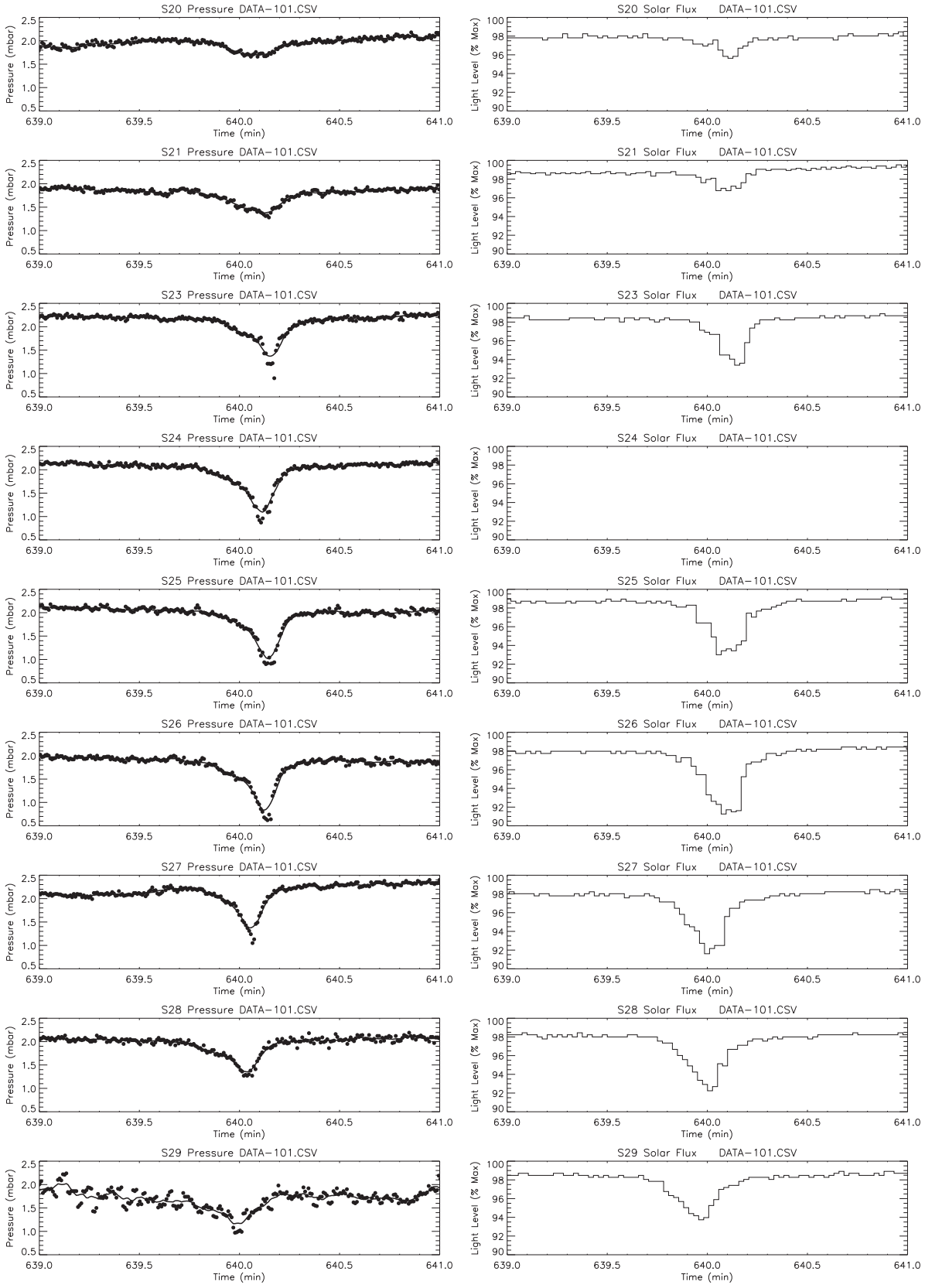

Fig. 6. A 'textbook' encounter, where a clean vortex signature is visible in all stations, but falls off to either side. The plots are a 2-min record from each station, with pressure (normalized to the beginning of the original datafile) plotted on the left, and solar flux (normalized to maximum) on the right. The devil is dust-laden, as evidenced by the sunlight drop that is simultaneous with the pressure signal. Note that no solar data is available on station S24. Station S22 failed and is not shown – there is therefore a larger spatial distance between the second and third row of plots than the others; the data from station S29 is unaccountably noisier than the others, but is still usable. Data from this encounter are compared with an analytic model in Fig. 10. Note that the profile is asymmetric – the attack is shallower and longer than the decay.

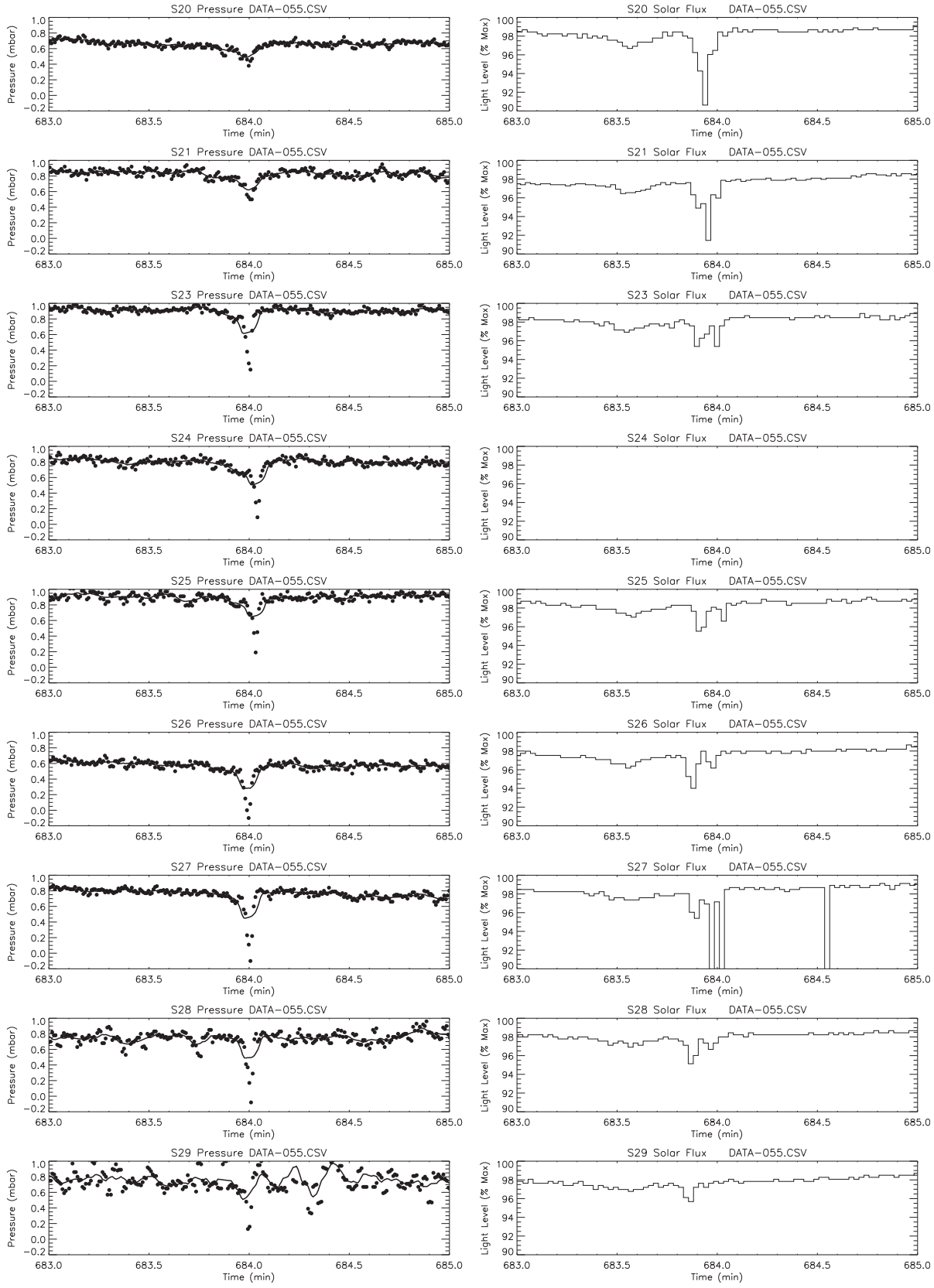

Fig. 7. An encounter with a fairly narrow devil – the raw signature is less than 10 s long, but is rather intense, with a ~1 mb core pressure drop at S27. It is notable that the obscuration signal has a pronounced double dip, suggesting a well-defined dust wall with a clear central region.

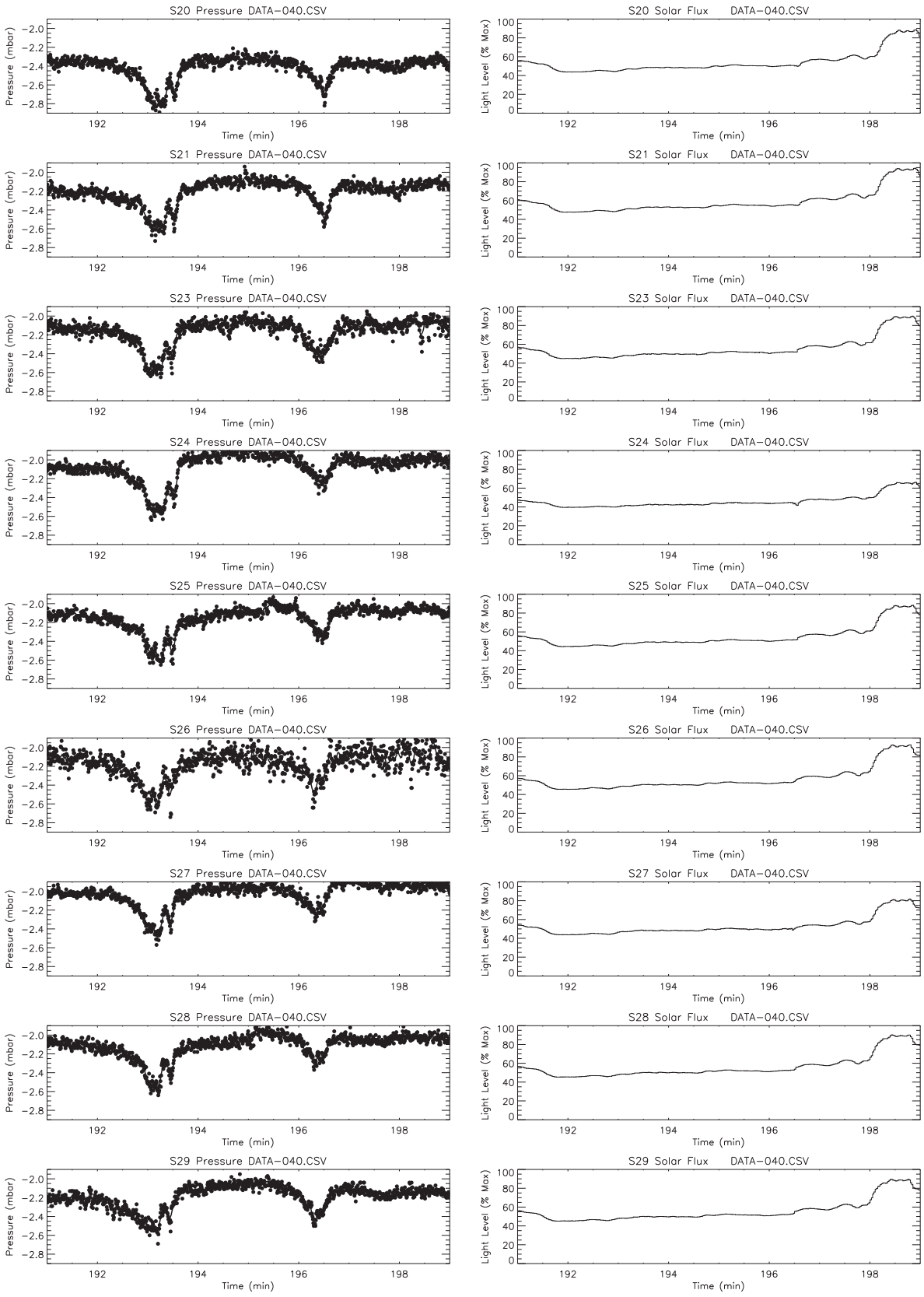

Fig. 8. An encounter with a pair of vortices (or possibly a single cycloidally-migrating devil) on a cloudy day. Although difficult to discriminate against the overall light level variation, a distinct dip in light level is seen in most stations at 192.5 min, coincident with the edge of the first pressure dip. A short and localized dust blockage is seen in stations S24 and S27 at 195.5 min.

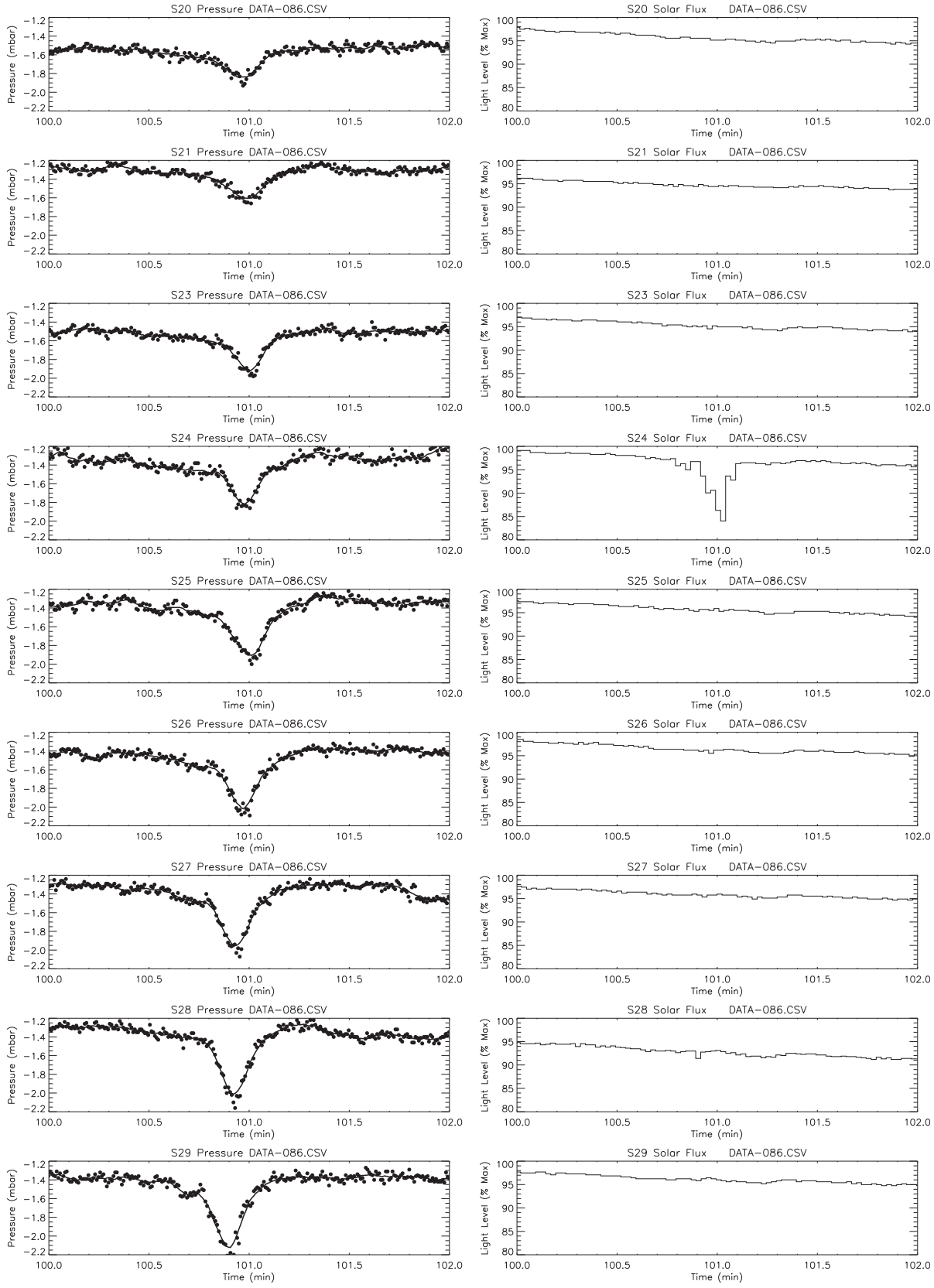

Fig. 9. A pleasingly well-measured encounter, albeit one where the pressure disturbance extends beyond the range of the array – the maximum excursion observed is at S29, so the vortex crossed the array line between S28 and S29, or somewhere beyond S29. Notable in this instance is the very small drop in light level seen in most stations, but a very significant one in the S24 record: possible explanations are discussed in the text.

encounters. It is seen in LES (Large Eddy Simulations) of boundary layer convection (e.g., Raasch and Francke, 2011) that vortices tend to form at the upwelling corners of convection cells, which tend to have a dimension comparable with the height of the atmospheric boundary layer (typically of the order of 1–2 km in summer afternoons). Thus one might expect a characteristic interval of dust devil occurrence to be 200–1000 s if the ambient wind advecting the convection pattern is 2–5 m/s, and indeed 10–20 min periodicities are sometimes noticed in records of dust devil activity (Carroll and Ryan, 1970; Lorenz and Lanagan, 2014). However, smaller cells, faster advection, and multiple vortices along the edge of a cell rather than just at a corner, could all lead to encounters spaced, as here, by only a minute. On the other hand, if the ambient wind is very low, a dust devil may perform cycloidal excursions (Lorenz, 2013) rather than a straight-line path, resulting in multiple close encounters and thus multiple dips in a single-station pressure record.

The first encounter has a pronounced subsidiary dip after the main part. If this were in a single record it might be interpreted as suggesting a multi-core vortex. The fact that this short event appears consistently in every record argues against a small feature (i.e. its influence spans some 40 m).

Fig. 9 shows another high-quality encounter (like Fig. 7) but in this instance the center of the vortex is at or beyond the end of the array and the maximum excursion observed is at S29. The encounter is slightly asymmetric, although with a slightly different character from Fig. 7, with a shallow linear attack portion (perhaps due to a curved trajectory) before a break in slope to the main pressure dip. A prominent ~15% dip in solar flux is seen only at station S24 suggesting a highly variable dust loading. The lack of a distinct pressure signature in this record beyond a smooth profile intermediate between that of S23 and S25 argues against some sort of subsidiary vortex structure – it may be that the local dust availability is higher due to less grass cover or some similar effect.

It is clear from these results that an array measurement is a powerful technique for assessing the nature of individual encounters, and interpretations can be considerably more secure than those of individual pressure records. A linear array as here has some ambiguities, especially given fluctuations in real-world devils, that make detection of fine structure (e.g., multiple-core vortices – see e.g., Snow et al. (1980)) so future experiments with two-dimensional arrays will be interesting. In the next section we examine a couple of the recorded events in more detail and compare with analytic models of vortices.

6. Quantitative analysis of array measurements

The development of horizontally-distributed measurement of dust devil meteorological data is novel, offering many possible investigations and we will attempt only some brief analyses here. The data shown in plots 6–9 is made available at http://pds-atmospheres.nmsu.edu/data_and_services/atmospheres_data/Field_and_Lab/dustdevils.html: and as Supplemental information to this paper. The rather voluminous raw data is available from the first author upon request.

An obvious question is whether these array data can effectively solve for the core pressure drop and diameter of a vortex. Following Lorenz (2014), we use a succinct analytic vortex model, originally due to Vatistas et al. (1991)) which gives excellent agreement with laboratory data and avoids the undifferentiable (and unphysical) singularity at the wall in the idealized Rankine model of the 1880s. Lorenz (2014) showed this model gives an excellent agreement of the velocity-distance measurements of a dust devil in the field by Tratt et al. (2003). The model has the following functions of tangential velocity and pressure as a function of normalized distance r ($r = 2z/d$, with z being the horizontal coordinate from center, and d the vortex wall diameter).

$$V_t = V_o(r/(1+r^4)^{0.5}) \quad (1)$$

$$\Delta P_{obs}(x) = \Delta P_o\{1 - (2/\pi)\arctan(r^2)\} \quad (2)$$

where V_t is the tangential wind velocity and V_o is the wind scaling speed (the maximum tangential windspeed, that at the wall, is equal to $V_o/2^{1/2}$). ΔP_{obs} is the observed pressure at station x and ΔP_o is the core pressure drop. Clearly, while more realistic than the Rankine model used in some prior studies, this is nonetheless an idealization, not least for possible multi-core vortices. An important objective in future work with a larger set of vortex records would be to explore which analytic functions best describe the pressure fields of real dust devils (e.g., Ellehoj et al., 2010 empirically chose a Lorentzian function). Nonetheless, the Vatistas model above provides a convenient basis for examination of the field data. A feature of this model (and indeed most analytic models) is that the pressure drop at the wall of the vortex is equal to half that at the core.

The data of Fig. 6 is replotted in Fig. 10 along with a model prediction based on Eq. (2) above. It is assumed the dust devil moves at a uniform speed v in the y-direction, where y is orthogonal to the array. The devil crosses the array ($y = 0$) at an intercept x_c (where x is measured along the array from S20) and time t_0. Thus $y(t) = v(t - t_0)$, and for each station N $z_N(t) = [y^2 + (x_c - x_N)^2)^{1/2}$. The coordinates x_N are measured from just beyond the western end of the array, thus for $N = [\text{“S20”}, \text{“S21”} \ldots \text{“S29”}]$ we have $X_N = [0, 4, \ldots 36]$.

It can be seen that by choosing appropriate values of v, the wall diameter d and core pressure drop ΔP_o and intercept coordinate x_c that the Vatistas model describes the observed pressure time histories rather well. It is evident by inspection that $20 < x_c < 24$ m since the greatest pressure drops were seen at stations S25 and S26. Model diameters of 18 to 24 m and core pressure drops of 1.3 to 1.6 mbar bound the data, so a best estimate might be ~21 m and 1.45 mbar.

In essence, this exercise is a parametric estimation problem. We have five principal unknowns, namely the core pressure drop and diameter of the devil, its two-dimensional advection velocity, and the coordinate at which it crosses the array line. We must estimate these unknowns with the data at hand, namely the pressure time series from the stations, plus any other ancillary information. As noted previously, for a single station record alone, we cannot unambiguously solve for all these parameters, or even for a slightly reduced set invoking the radial symmetry of the problem. If the wind speed and direction are known (and the dust devil translation velocity assumed to be equal to that of the wind – which may not be completely accurate – see e.g., Balme et al., 2012) the situation is improved, but still does not collapse the estimate completely. An array provides additional data, solving for the crossing point by inspection when the devil crosses the array.

The fit could be improved by slight adjustments of the time and pressure offsets for each record – these could be shifted to force exact coincidence of the time of peak (i.e. minimum distance from center for all records) and to force a zero reading at the beginning of the record. Or one could instead allow these offsets to be free parameters, and optimize the least-squares error of the model, but this would greatly complicate the fitting procedure. It should be noted also that forcing coincidence of the peak is an assumption, essentially assuming that the dust devil moves normal to the array (i.e. forcing the x-component of velocity to zero).

In principle, although less accurate, the fit can be performed even when the crossing point is beyond the extent of the array, as was observed in Fig. 9. Because the core region, where the pressure drop is steepest, was not observed, there is some ambiguity between core pressure drop, diameter and miss distance (although less ambiguity than for a single station, obviously).

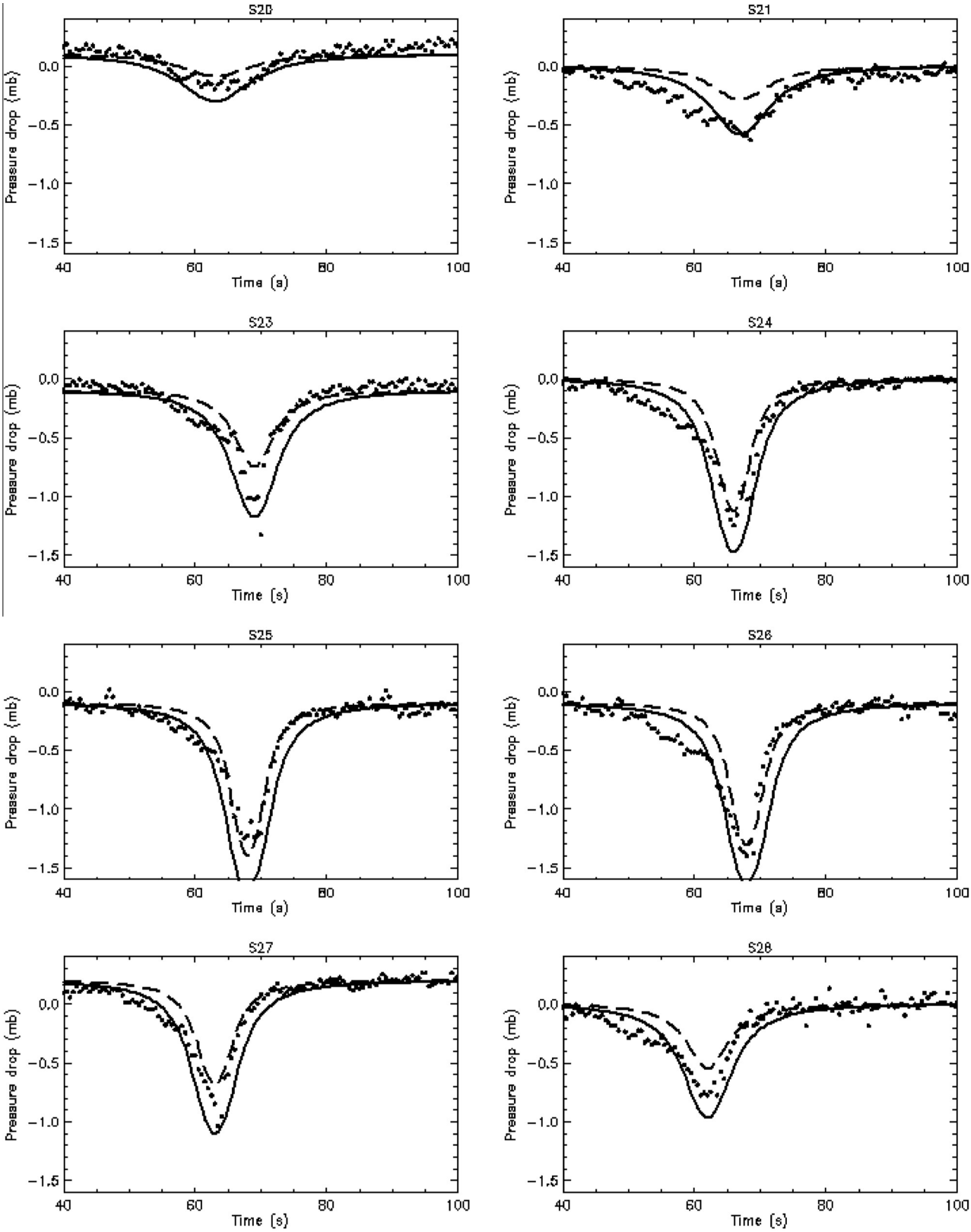

Fig. 10. The encounter in Fig. 6 plotted against the analytic vortex model described in the text. The model parameters for the solid and dashed curves respectively, which appear to bound the data well are diameters of 20 m and 15 m and core pressure drops of 1.3 mbar and 1.6 mbar. Note that the symmetric model does not reproduce the early onset of the pressure drop. The noisy S29 data are not shown.

Finally, we note that in some instances the solar data solves one unknown for us. Specifically, the well-defined optical wall seen in the encounter in Fig. 7 provides a direct estimate of the dust devil diameter, in that the two dips in light intensity are 6 s apart in several records. We can furthermore observe that at the extreme ends of the array, the optical signature is a single dip indicating a tangential encounter, and thus we may estimate the diameter at ~40 m. The implication, assuming an axisymmetric vortex, is of

an advection speed of 6–7 m/s to force the two diameters to be equal.

In future work we will explore the retrieval of dust devil population parameters using numerical simulations. Such work can evaluate the information contributed by each element in an array and thereby determine the optimum instrumentation configuration for a given dust devil population. Critical in that study will be the assumed direction diversity of dust devil migration. If dust devils move in all azimuths, a more equant (square or circular) array would be preferred, whereas if all dust devils move in a single direction – the assumption made in this initial deployment – then a more stretched (rectangular) array would be more efficient in terms of maximizing number of encounters per unit time. It may also be noted that while an equant array yields a smaller 'harvest' of encounters, it solves the encounter direction problem and allows a full 2-D characterization of the pressure field.

7. Conclusions

We have made the first quantitative surveys of dust devil activity at La Jornada. The dust devil vortex population (~0.5 events/day) measured by 6s-average pressure drops of 0.2 mbar or higher in May/June 2013 appears to be a factor of a few lower than that recorded for similar drops at El Dorado in Nevada the previous summer – meteorological conditions are no doubt a major factor – but the vortex population distribution is of a similar shape.

We have furthermore made the first pseudo-2-D measurements of dust devil horizontal structure, using a linear array of sensor stations and exploiting the dust devil migration to 'section' itself on the array. A simple analytic vortex model describes the 2-D pressure field rather accurately, and offers the possibility to independently measure the size and depth of the pressure well. Some azimuthal variations are seen, notably a leading/trailing asymmetry, likely related to the fluid mechanics associated with the advection of the vortex. Solar cell data provides insight not only on the dust loading of an individual vortex, but also in some cases provides an accurate and independent measure of the wall diameter, as well as some insight into the advection direction.

Some important lessons have been learned for future array measurements. First, raising the loggers off the ground is desirable to avoid waterlogging – a remarkably prevalent hazard given the desert application. Similarly, some sort of restraint to avoid overturning is useful, but of course, the logistical effort involved in securing each station must be weighed against the large effort involved in applying such procedures to large numbers of stations.

Second, an important ambiguity exists in a line array if data are not synchronized within a few seconds, namely that a devil of a given diameter can 'seem' much larger if it encounters at an oblique angle. If data are ad-hoc synchronized to match the peak pressure drop time, the discrimination between a small devil at an oblique angle and a normal encounter with a larger devil is lost. Nearby and synchronized windspeed and direction information (useful for other reasons) would also help resolve this ambiguity. Another approach would be to have a parallel line, perhaps with fewer stations more widely spaced, to determine two E–W intercept coordinates and thus determine the azimuth of migration.

Clearly, many tradeoffs exist in choosing the optimum deployment configuration of a given set of stations – a wider spacing is more efficient at 'harvesting' the maximum number of detections, but a narrower spacing better resolves horizontal structure, and so on. Data now available to constrain population evolution models (Lorenz, 2014) will permit such optimizations to be performed in silico, prior to making a deployment.

Acknowledgements

This work was funded by NASA through the Mars Fundamental Research Program grant number NNX12AI04G. RL thanks Brian Jackson of Boise State University for assistance with previous but less successful array measurement attempts. We thank the Astronomy Department of NMSU for assistance with shipping and the NASA Planetary Data System Atmospheres Node for hosting dust devil data.

Appendix A. Supplementary data

Supplementary data associated with this article can be found, in the online version, at http://dx.doi.org/10.1016/j.aeolia.2015.01.012.

References

Balme, M.R., Hagermann, A., 2006. Particle lifting at the soil–air interface by atmospheric pressure excursions in dust devils. Geophys. Res. Lett. 33, L19S01. http://dx.doi.org/10.1029/2006GL026819.

Balme, M.R., Pathare, A., Metzger, S.M., Towner, M.C., Lewis, S.R., Spiga, A., Fenton, L.K., Renno, N.O., Elliott, H.M., Saca, F.A., Michaels, T.I., Russell, P., Verdasca, J., 2012. Field measurements of horizontal forward motion velocities of terrestrial dust devils: towards a proxy for ambient winds on Mars and Earth. Icarus 221, 632–645.

Carroll, J.J., Ryan, J.A., 1970. Atmospheric vorticity and dust devil rotation. J. Geophys. Res. 75, 5179–5184.

Ellehoj, M.D., Gunnlaugsson, H.P., Taylor, P.A., Kahanpää, H., Bean, K.M., Cantor, B.A., Gheynani, B.T., Drube, L., Fisher, D., Harri, A.-M., Holstein-Rathlou, C., Lemmon, M.T., Madsen, M.B., Malin, M.C., Polkko, J., Smith, P.H., Tamppari, L.K., Weng, W., Whiteway, J., 2010. Convective vortices and dust devils at the Phoenix Mars mission landing site. J. Geophys. Res. 115, E00E16.

Karstens, C.D., Samaras, T.M., Lee, B.D., Gallus Jr., W.A., Finley, C.A., 2010. Near-ground pressure and wind measurements in Tornadoes. Mon. Weather Rev. 138, 2570–2588.

Lambeth, R.L., 1966. On the measurement of dust devil parameters. Bull. Am. Meteorol. Soc. 47, 522–526.

Lorenz, R.D., 2008. A 20-station array of intelligent dataloggers to study dust devils: preliminary trials. In: XXXIXth Lunar and Planetary Science Conference, Houston, TX, March 2008 (Abstract #1382).

Lorenz, R.D., 2012a. Pressure drops in dust devils: Earth and Mars. Planet. Space Sci. 60, 370–375.

Lorenz, R.D., 2012b. Observing desert dust devils with a pressure logger. Geosci. Instrum. Methods Data Syst. 1, 209–220.

Lorenz, R.D., 2013. Irregular dust devil pressure drops on Earth and Mars: effect of cycloidal tracks. Planet. Space Sci. 76, 96–103.

Lorenz, R.D., 2014. Vortex encounter rates with fixed barometer stations: comparison with visual dust devil counts and large eddy simulations. J. Atmos. Sci. 71, 4461–4472.

Lorenz, R.D., Lanagan, P.D., 2014. A barometric survey of dust devil vortices on a Desert Playa. Bound. Lay. Meteorol. 53, 555–568.

Lorenz, R.D., Jackson, B.K., 2015. Dust devils and dustless vortices on a Desert Playa observed with surface pressure and solar flux logging. GeoResJ 5, 1–11.

Murphy, J., Nelli, S., 2002. Mars pathfinder convective vortices: frequency of occurrence. Geophys. Res. Lett. 29, 2103.

Raasch, S., Franke, T., 2011. Structure and formation of dust devil-like vortices in the atmospheric boundary layer: A high resolution numerical study. J. Geophys. Res. 116, D16120. http://dx.doi.org/10.1029/2011JD016010.

Ringrose, T.J., Patel, M.R., Towner, M.C., Balme, M., Metzger, S.M., Zarnecki, J.C., 2007. The meteorological signatures of dust devils on Mars. Planet. Space Sci. 55, 2151–2163.

Sinclair, P.C., 1973. The lower structure of dust devils. J. Atmos. Sci. 30, 1599–1619.

Snow, J.T., McClelland, T., 1990. Dust devils at white sands missile range, New Mexico 1. Temporal and spatial distributions. J. Geophys. Res. 95, 13707–13721.

Snow, J.T., Church, C.R., Barnhardt, B.J., 1980. An investigation of the surface pressure fields beneath simulated tornado cyclones. J. Atmos. Sci. 37, 1013–1026.

Tratt, D.M., Hecht, M.H., Catling, D.C., Samulon, E.C., Smith, P.H., 2003. In situ measurement of dust devil dynamics: toward a strategy for Mars. J. Geophys. Res. (Planets) 108 (5116), 1–7. http://dx.doi.org/10.1029/2003JE002161.

Vatistas, G.H., Kozel, V., Mih, W.C., 1991. A simpler model for concentrated vortices. Exp. Fluids 11, 73–76.

Wyett, R.E., 1954. Pressure drop in a dust devil. Mon. Weather Rev. 82, 7–8.